Tears of Venom: Hydrodynamics of Reptilian Envenomation

Bruce A. Young,[1] Florian Herzog,[2] Paul Friedel,[2] Sebastian Rammensee,[2] Andreas Bausch,[2] and J. Leo van Hemmen[2]
[1]*Anatomical Laboratory, Department of Physical Therapy, University of Massachusetts, Lowell, Massachusetts 01854, USA*
[2]*Physik Department, Technische Universität München, 85747 Garching bei München, Germany*
(Received 26 September 2010; revised manuscript received 29 January 2011; published 12 May 2011)

In the majority of venomous snakes, and in many other reptiles, venom is conveyed from the animal's gland to the prey's tissue through an open groove on the surface of the teeth and not through a tubular fang. Here we focus on two key aspects of the grooved delivery system: the hydrodynamics of venom as it interacts with the groove geometry, and the efficiency of the tooth-groove-venom complex as the tooth penetrates the prey's tissue. We show that the surface tension of the venom is the driving force underlying the envenomation dynamics. In so doing, we explain not only the efficacy of the open groove, but also the prevalence of this mechanism among reptiles.

DOI: 10.1103/PhysRevLett.106.198103 PACS numbers: 87.85.gf, 47.20.Dr, 47.50.−d, 47.60.Dx

Functional bases, clinical consequences, and phylogeny of envenomation by snakes have been studied extensively. Nevertheless, the underlying biological physics is poorly understood. This likely stems from a skewed perspective as previous literature has concentrated on a minority of venomous snakes (like rattlesnakes [1]) that use tubular fangs to rapidly inject a pressurized bolus of venom. In the majority of venomous snakes, and in several other groups of venomous reptiles, envenomation is a very different process [2–4]. In these species venom is released with little or no pressure head, essentially it oozes in the vicinity of one or more enlarged grooved fangs (Fig. 1) with which the snake slowly and repeatedly penetrates the prey tissue. Previous studies [5,6] have shown that, to be effective, reptilian venom must be introduced below the epidermis (the surface layer of the organism) and that, as a generality, the efficacy of envenomation is directly proportional to the volume and depth of the venom released. Why, then, use a groove?

Here we offer a biophysical explanation for the importance of the fang's groove as a venom conduit. We also detail how the penetration of prey tissue by the grooved fang creates a "venom tube" bordered by the topography of the groove as well as the disrupted tissue of the prey; cf. Fig. 1(b). The venom tube both effectively extends the fang's groove below the epithelium and, through surface tension in conjunction with non-Newtonian behavior as detailed below, increases the efficacy of envenomation by drawing the venom into the prey.

As part of our biophysical explanation of envenomation, we now address three, related, questions. First, what qualities characterize venom as a fluid? Second, how does the venom oozing out of the gland "flow" along the fang's groove? And third, how does the complex of tooth-groove-venom behave as the tooth penetrates into the prey's tissue? By quantifying the venom viscosity η as a function of the shear rate, we document that the venom is a non-Newtonian fluid. We quantify the venom's surface tension and show how this surface tension spreads the venom along the fang's groove forming a stable composite system between the venom and the topography of the fang. Both the venom spreading along the fang's groove and its penetration into the target tissue arise through a minimization of the venom's surface-tension energy. As Fig. 2 below shows, the larger the shear tension produced by fang penetration, the more fluid the venom is. Predicted rates of venom flow along the groove and into the prey (i.e., absorption between 0.1 and 1 s) are similar to what has been observed during feeding of snakes [7].

To determine surface tension and viscosity, fresh venom was obtained by milking a western diamondback rattlesnake (*Crotalus atrox*) and a red spitting cobra (*Naja pallida*). Venom drops were photographed, along with water droplets, on glass slides and teeth, in order to

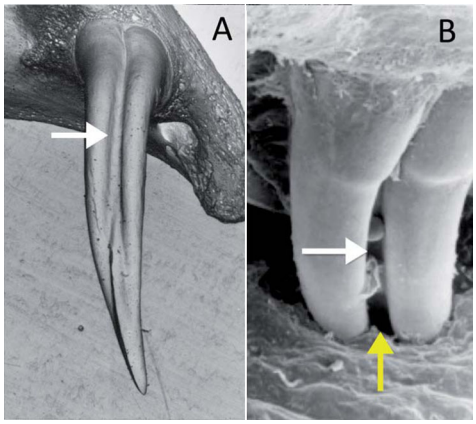

FIG. 1 (color online). Scanning electron micrographs showing the prominent grooves (horizontal arrows) on the fangs of (a) a banded snake (*Bothryum lentiginosum*), a lizard eater, and (b) a mangrove snake (*Boiga dendrophila*), a generalist feeding on both birds and lizards. The Boiga specimen was prepared with the fang imbedded in prey tissue, so only the base of the fang is visible; the prey tissue has separated slightly from the fang forming a clear venom tube (vertical arrow).

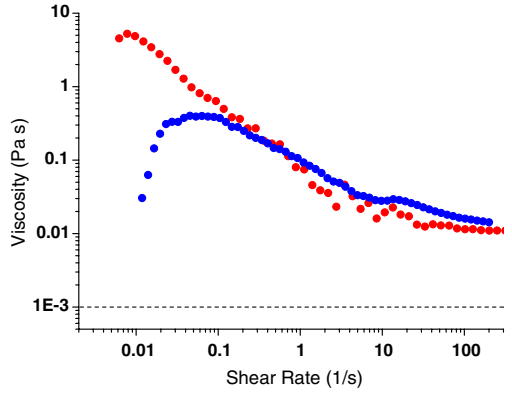

FIG. 2 (color online). Graph of viscosity as a function of shear rate for venom (blue trace) and a 50:50 mix of venom and saliva (monotonically decreasing, red trace), double-logarithmic scale. Both samples show a distinct shear-thinning behavior, which is typical for non-Newtonian polymer solutions. For comparison, water (horizontal, dashed black line) is a Newtonian fluid where the viscosity does not depend on the applied shear rate.

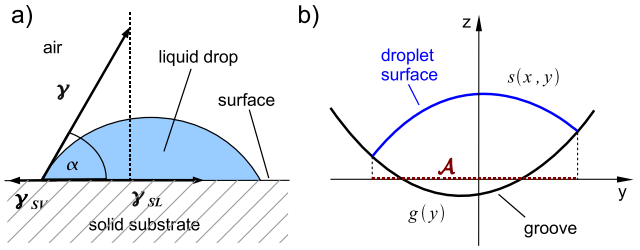

FIG. 3 (color online). (a) Schematic of the surface tensions acting on a venom droplet; in principle they are vectors. The contact angle α is formed through the interactions of two surface tensions, one between the venom and the air (γ), and the other (γ_{SL}) between the venom and the substrate, here the fang. The third surface tension γ_{SV} between substrate and venom vapor effectively vanishes and we choose units so that $\gamma = 1$. (b) A venom droplet in a groove parallel to the x axis, which is orthogonal to the plane, is bounded by the function $g(y)$ and by the venom-air surface $s(x, y)$.

determine the contact angle (defined and explained below), which was approximately 45°. Quantification of 30 μl drops of *C. atrox* venom and a 50:50 mix of venom and saliva yielded surface-tension values of 49.5 and 52.2 mN/m, respectively, which are slightly below that of water (viz., 73 mN/m). The surface-tension quantification (sessile-drop technique), as well as the rheological experiments described below, were all done at 20 °C.

Both the *C. atrox* venom and (for biological realism) a 50:50 mix of venom and saliva have relatively high viscosities compared to water (cf. Fig. 2), meaning that venom would flow relatively slowly (~ 1 cm/s) over the tooth. This rate is consistent with what is observed biologically: snakes with grooved teeth release venom relatively slowly (with little, or no, pressure head) while holding, and often repeatedly penetrating, prey with their teeth [11]. This is in sharp contrast to the rapid pressurized bolus of venom that is passed by snakes with tubular fangs [8]. As shown in Fig. 2, the venom is a non-Newtonian fluid (the viscosity η changes with shear force), the flow rate of which accelerates when the tooth penetrates a prey item, producing shear.

Measuring the contact angle α precisely is not an easy task—see Fig. 3(a) for a pictorial definition—because it is strongly influenced by factors such as the presence of impurities or small surface features which amply occur in biological reality. Fortunately, it is not necessary to know the exact value of the contact angle but only whether the angle is much smaller than 90°, much larger than 90°, or just about 90°. In the first case, the fluid tends to spread over a surface, and in the latter case it tends to contract and form a spherical droplet. Snake venom clearly belongs to the first category. That is, a venom's contact angle is comparable with that of water (being much smaller than 90°) but its viscosity is 2 orders of magnitude higher. Hence snake venom flows roughly 500 times more slowly than water [9] but, as it turns out, this flow rate is fast enough.

Now we know both viscosity and surface tension we can turn to the question of how venom distributes itself in the groove once it has been released by the venom gland. In Fig. 3(a) we see a drop in equilibrium. Forces between molecules hold the liquid together and influence the shape of the drop. The molecules on the surface of the drop are acted upon by forces from the inside of the drop and different ones (or none) on the other side. A droplet tends to minimize its surface to establish a force equilibrium, a behavior that can be described quantitatively by introducing a potential energy, the surface energy, which is proportional to the size of the surface A: $E = \gamma|A|$. The proportionality factor γ has dimension N/m and is therefore called the surface tension, a material constant.

For the situation of Fig. 3(a) we have three kinds of surface tension, γ, γ_{SV}, and γ_{SL}, indicating the interaction at the surfaces venom-air, solid-vapor, and solid-liquid (or tooth-venom). All three are actually vectors but will be treated as scalar substitutes. Because of momentary equilibrium, their sum vanishes so that

$$\gamma \cos\alpha + \gamma_{SL} = \gamma_{SV}. \quad (1)$$

We set $\gamma = 1$ [or divide (1) by γ]. Since $\alpha \approx 45°$ and, effectively, $\gamma_{SV} = 0$ we end up with $\cos\alpha = -\gamma_{SL}$. That is, $\gamma_{SL} < 0$ and the interface between venom and tooth effectively tends to get *maximized*.

The groove in the fang is taken to be translationally invariant (for the purpose of a venom drop getting dispersed) with a preferred axis along the x axis. Accordingly, we need only specify the intersection as indicated in Fig. 3(b) where the groove's bottom is given by a function $g(y)$ while the venom surface is represented by a function $s(x, y)$ so that $s(x, y)$ will depend not only on y but also on x as we move along the tooth. The same in principle holds for g but in practice this is not relevant, as detailed below. So

the venom is contained in a volume bounded "below" by g and "above" by s. This allows us to specify a minimization problem.

The energy functional E_{surface} that is to be minimized is the total energy incorporating all the surface tensions (with $\gamma = 1$), viz., the surface integral

$$E_{\text{surface}} = E_{\text{venom-air}} + E_{\text{venom-tooth}} = \int_{\mathcal{A}} dxdy\sqrt{1 + s_x^2 + s_y^2} + \gamma_{\text{SL}} \int_{\mathcal{A}} dxdy\sqrt{1 + g_x^2 + g_y^2}. \quad (2)$$

Here, $\mathcal{A}$ is the region enclosed by the projection of the venom-tooth boundary onto the (x, y) plane that defines our integration boundary [see Fig. 3(b)] while the lower index x in, e.g., s_x means a partial derivative with respect to x and analogously for y. Furthermore, in minimizing (2) the total volume of the venom is conserved and thus so is

$$\int_{\mathcal{A}} dxdy[s(x, y) - g(x, y)] = C^{\text{st}}. \quad (3)$$

The above minimization problem is rather intricate in that the venom can float freely in the groove and hence the boundary $\partial\mathcal{A}$ of the region $\mathcal{A}$ is free to move as well. Figure 4(a) shows this is exactly what happens. To obtain solutions to the minimization problem (2) under the constraint (3) with free boundary $\partial\mathcal{A}$ we have taken advantage of special software called SURFACE EVOLVER [10]. SURFACE EVOLVER discretizes the droplet surface via triangularization and adjusts the surface shape stepwise to minimize surface energy numerically. To model the groove more precisely it was built up as a combination of a convex and a concave arc with radius R_1 and R_2, respectively, and an angle β to locate the transition between convex and concave; cf. Fig. 4(c).

In general, venom oozes out of the gland. As shown in Fig. 4(a), a venom droplet placed on different dental surfaces always moves "down" into the groove even though gravity has been neglected here since for a realistic snake tooth the R's are smaller than the capillary length $\lambda_c = \sqrt{\gamma/(\rho g)}$ [9]. Phrased differently, a venom drop is stretched in the direction parallel to the groove and contracts in the orthogonal direction. That is why it is advantageous to model the two-dimensional intersection generating the three-dimensional groove by means of three curves, two convex ones on the upper left and right and a central concave one; varying the radii of the curves changes the width of the groove, whereas varying the angle β [see Fig. 4(c)] of the two positions where the three curves meet alters the depth of the groove. The contours of the groove allow maximization of the substrate contact with the venom droplet while minimizing the surface area of the droplet exposed to the air; as such, the grooved configuration allows the venom droplet to also achieve minimal (negative) surface energy ($E_{\text{venom-tooth}}$), respecting the constant-volume constraint (3). The results of these simulations are consistent in that venom droplets flow over the surface of the tooth so as to move into the groove, a displacement that is more pronounced with increasing groove depth, as indicated clearly in Fig. 4(b).

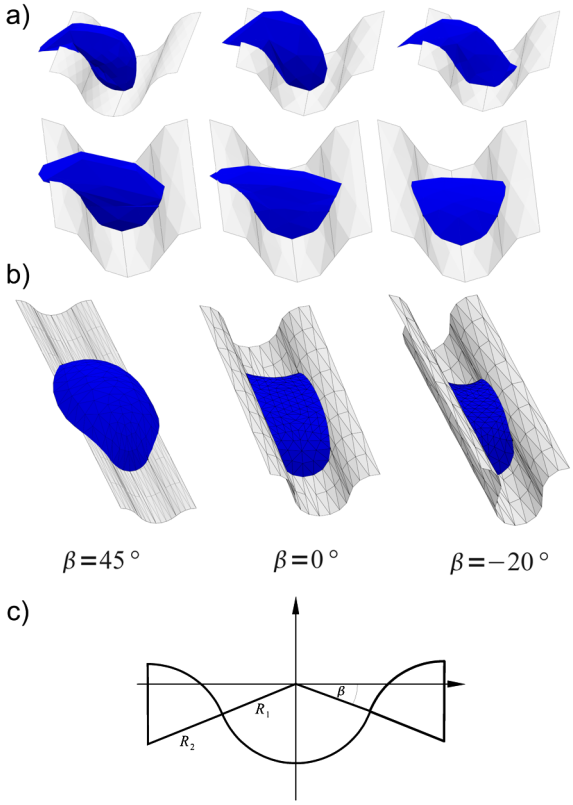

FIG. 4 (color online). Results of a numerical minimization of (2) under the constraint (3) with free boundary $\partial\mathcal{A}$ in which the surface area of the venom is modeled by a series of small intersecting triangles (triangularization) and the tooth as a translation of intersecting convex and concave curves. (a) A venom droplet flows over the surface of the tooth in order to enter the groove. Each stage in this sequence confers a lower surface-tension energy as given by (2). (b) Once in the groove, venom quickly spreads out (i.e., flows) along the length of the groove; this spread is directly related to a groove's contour and depth, with the *final* state shown for three different depths. We see the final state in dependence upon the groove angle β; cf. Fig. 1. (c) Grooves are modeled by two arcs of radius R_1 and R_2 (here $R_1 = R_2$); the angle of intersection β indicating the direction of the transition between convex and concave arcs determines a groove's shape and depth.

We now focus on three key findings. First, as noted above, once deposited in the groove by the venom gland, venom is attracted by a convex or convex-concave groove and drawn into it. For snakes feeding mainly on birds, β is indeed rather small, say $\beta = -20°$ in Figs. 1(b) and 4(b), so that feathers hardly wipe off the venom. Second, the venom spreads along the groove at an approximate rate $V^* = \gamma/\eta$ [9], where γ is the surface tension and η is the venom viscosity as shown in Fig. 2. For water this rate is as high as 70 m/s, while for snake venom it is in the range of 1 cm/s, agreeing with biological reality.

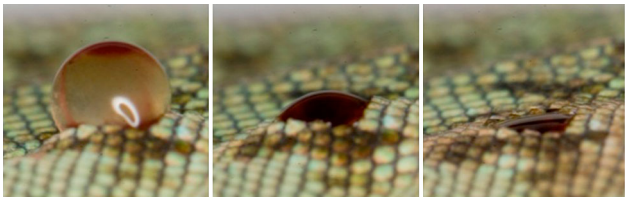

FIG. 5 (color online). Sequential photographs (covering a time span of less than 400 ms) showing a drop of venom from *Crotalus atrox* that was placed over a puncture wound on the lateral surface of an euthanized *Anolis* lizard. The venom droplet changes in shape and quickly penetrates into the tissue of the lizard.

With growing depth of the canal there is a certain point where it is better for a truly big drop to—so to speak—completely spread out along the canal independently of the drop volume. This happens when the contact area is much bigger than the free drop surface so that the sum of the two surface energies becomes negative at every drop volume. Estimating what is going to happen on the basis of $\cos\alpha = -\gamma_{SL}$ and (2) we then require, respecting (3),

$$E_{\text{surface}} = E_{\text{venom-air}} + E_{\text{venom-tooth}} = |\mathcal{A}_{\text{surface}}| - \cos\alpha|\mathcal{A}_{\text{contact}}| < 0. \quad (4)$$

Here, $\mathcal{A}_{\text{surface}}$ is the two-dimensional venom-air manifold, $\mathcal{A}_{\text{contact}}$ is the contact area between venom and tooth, another manifold, and α is the contact angle of Fig. 3. We see from Fig. 4 that the inequality (4) is indeed the driving principle as β decreases. The larger the contact angle α ($\cos 0° = 1$ and $\cos 90° = 0$) the deeper a groove has to be to realize the above inequality. For comparison, on a flat (nongrooved) tooth we always have $|\mathcal{A}_{\text{surface}}|/|\mathcal{A}_{\text{contact}}| > 1$. The venom-spreading function of the groove is a consequence of the surface tension of the venom as represented by $\cos\alpha$.

Third, and finally, what happens if the system of grooved tooth and venom covering the groove is pushed into prey tissue [12]? Groove and tissue then form a tubular construct through which venom is soaked in so as to obey surface tension. More precisely, the exposed wound, like the groove on the surface of the tooth, represents an increased surface area that minimizes the surface energy of the venom and functions to draw the venom in. Following tooth penetration, the combination of dentitional groove and the (disrupted) skin of the target will form what is effectively a venom tube extending into the target tissue.

As shown in Fig. 5, because of its surface tension venom on the surface of the tooth will be pulled into the groove and, rapidly, down the venom tube into the target tissue with hardly any spillover. The characteristic time τ_{cap} required for this envenomation can be estimated by the upper bound $\tau_{\text{cap}} = 8\eta H/\rho g a^2$ [13], where η is the venom viscosity, ρ the venom density, g is the gravity constant, and a and H are the tube's diameter and length, respectively. Substituting the values for η (cf. Fig. 2) and ρ that we have determined and using known groove dimensions [4], we find envenomation times of less than 1 s, as in Fig. 5 and again in agreement with biological practice.

In summary, we have presented experimental results on snake venom's viscosity and surface tension and analyzed the ensuing consequences. On the basis of the convex-concave groove geometry we can explain how and why a groove—which most commonly occurs in nature—inserts venom into prey. Surface tension is the driving force dominating this way of envenomation. The underlying biophysics nicely explains two key aspects of venom injection through a groove. First, the shape of the groove and the stability of venom in the groove awaiting prey. And, second, the speed at which venom is drawn into the target along the tube formed by the inserted fang's groove and the prey tissue.

Part of the present research has been supported by the BMBF through BCCN Munich. Dr. Tatyana Svitova and the Radke Lab at UC Berkeley assisted with the surface-tension measurements.

[1] B. A. Young, M. Blair, K. Zahn, and J. Marvin, Anat. Rec. **264**, 415 (2001).
[2] H.-D. Suess, Nature (London) **351**, 141 (1991).
[3] B. A. S. Bhullar and K. Smith, J. Herpetology **42**, 286 (2008).
[4] B. A. Young and K. V. Kardong, Amphibia-Reptilia **17**, 261 (1996).
[5] W. Hayes, P. Lavin-Murcio, and K. V. Kardong, Toxicon **31**, 881 (1993).
[6] B. S. Gold, R. C. Dart, and R. A. Barish, New Engl. J. Med. **347**, 347 (2002).
[7] R. Thomas and J. A. Prieto-Hernandez, Dec. Simp. Rec. Nat. 13 (1983–1985).
[8] B. A. Young and K. Zahn, J. Exp. Biol. **204**, 4345 (2001), http://jeb.biologists.org/content/204/24/4345.full.
[9] P.-G. de Gennes, F. Brochart-Wyart, and D. Quéré, *Capillarity and Wetting Phenomena: Drops, Bubbles, Pearls, Waves* (Springer, New York, 2004).
[10] K. Brakke, The SURFACE EVOLVER: Exp. Math. **1**, 141 (1992), http://www.susqu.edu/brakke/evolver/evolver.html.
[11] K. Kardong and P. A. Lavin-Murcio, Copeia 644 (1993).
[12] T. Frazzetta, J. Morphol. **118**, 217 (1966).
[13] H. Bruus, *Theoretical Microfluidics* (Oxford University Press, Oxford, 2007); see, in particular, section 7.3.2.